Electronic Supplementary Material (ESI) for Physical Chemistry Chemical Physics.

Supporting Information

A *multi*donor-Photosensitizer-*multi*acceptor Triad for Long-Lived Directional Charge Separation

Tina Schlotthauer,[a] Robert Schroot,[a] Starla Glover,[b] Leif Hammarström,[b] Michael Jäger,[a,c,] and Ulrich S. Schubert[a,c,]**

[a] Laboratory of Organic and Macromolecular Chemistry (IOMC), Friedrich Schiller University Jena, Humboldtstraße 10, 07743 Jena, Germany

[b] Department of Chemistry - Ångström Laboratory, Uppsala University, Box 523, SE75120 Uppsala, Sweden

[c] Center for Energy and Environmental Chemistry Jena (CEEC Jena), Friedrich Schiller University Jena, Philosophenweg 7a, 07743 Jena

Content

1. Instrumentation 2
2. Syntheses 3
3. NMR spectroscopy 6
4. Mass spectrometry 12
5. Size-exclusion chromatography 14
6. Steady state optical data 16
7. Spectroelectrochemical data 17
8. Time-resolved data 18
8.1. Emission data 18
8.2. Transient absorption data 21

1. Instrumentation

NMR spectra were recorded on a 300 or 600 MHz NMR spectrometer (Bruker AVANCE or Fourier 300) in deuterated solvents at 300 K. Chemical shifts are reported in parts per million (ppm, δ scale) relative to the residual solvent signal.[1]

MALDI-TOF MS spectra were measured using an Ultraflex III TOF/TOF (Bruker Daltonics GmbH) equipped with a Nd:YAG laser and a collision cell. The spectra were recorded in the positive reflector or linear mode.

ESI-Q-TOF MS measurements were executed on a micrOTOF (Bruker Daltonics GmbH) mass spectrometer, which was equipped with an automatic syringe pump for sample injection. The pump was supplied from KD Scientific. It was operated in the positive ion mode. The standard electrospray ion (ESI) source was used to generate ions. Mixtures of dichloromethane and acetonitrile were used as solvent. The ESI-Q-TOF-MS instrument was calibrated in the m/z range 50 to 3,000 using an internal calibration standard (Tunemix solution), which was supplied from Agilent.

UV/Vis absorption spectra were measured on a Perkin-Elmer Lambda 45 UV/Vis spectrophotometer and emission as well as excitation spectra were recorded using a Jasco FP6500. Measurements were carried out using approx. 10^{-7} M solutions of aerated dichloromethane (spectroscopy grade) in 1 cm quartz cuvettes at 25 °C.

Flash column chromatography was carried out on a Biotage Isolera One System using Biotage SNAP Cartridges KP-Sil. The Biotage Initiator Sixty Microwave synthesizer was used for microwave reactions.

Preparative size exclusion chromatography was either performed by using Bio-Beads (S-X1, dichloromethane) or Toyopearl (HW-55F, CH_2Cl_2/MeOH 95/5).

Analytical size exclusion chromatography was performed on the following systems:
SEC1. Shimadzu system (controller: SCL-10A VP, degasser: DGU-14A, pump: LC-10AD VP, auto sampler: SIL-10AD VP, oven: Techlab, UV detector: SPD-10AD VP, RI detector: RID-10A, eluent: chloroform/iso-propanol/triethylamine [94:2:4], flow rate: 1 mL/min, temperature: 40 °C, column: PSS SDV pre/lin S column).
SEC2. Shimadzu system (controller: SCL-10A VP, degasser: DGU-14A, pump: LC-10AD VP, auto sampler: SIL-10AD VP, oven: CTO-10A VP, UV detector: SPD-10MA VP, RI detector: RID-10A, eluent: DMAc + 0.08% NH_4PF_6, flow rate: 1 mL/min, temperature: 40 °C, column: Phenomenex Phenogel guard/10^5 Å/10^3 Å)

Time-correlated single photon counting was performed on a Edinburgh Instrument (EPL405), equipped a Hamamatsu MCP-photomultiplier (R3809U-51) for detection of single photons as described previously.[2] The laser's pulse energy was (ca. 15 pJ, 77 ps pulses) and attenuated to a count rate of ca. 1% or less of the excitation frequency. Specific measurements were performed with 470 nm excitation with a repetition rate of 20 µs using a long pass filter (715 nm) or 3C1 Russian Filter which transmits light at λ_{max} 540 with FWHM ca. 100 nm.[3] The IRF has not been deconvoluted from the traces.

Time-resolved flash photolysis measurements were made with a frequency tripled Q-switched Nd:YAG laser (from Quantel, brilliantB) where 355 nm pulses with a 7 ns duration were directed through an OPO tuned to output of 500 or 532 nm at ca. 10-20 mJ/pulse. Analyzing light was supplied by a pulsed 150

W xenon lamp in a flash photolysis spectrometer (Applied Photophysics, LKS.80). Light that passed through the sample was sent through a monochrometer set to a bandwidth of 7 nm prior to reaching the 5 stage P928 photomultiplier tube (Hamamatsu). The signal was digitized using an Agilent Technologies Infiniium digital oscilloscope (600 MHz). Transient absorption traces were generated within the Applied Photophysics LKS software package where rates for each sample condition were determined from 24–64 laser shots. All emission measurements were performed in 1 × 1 cm quartz cuvettes in DCM.

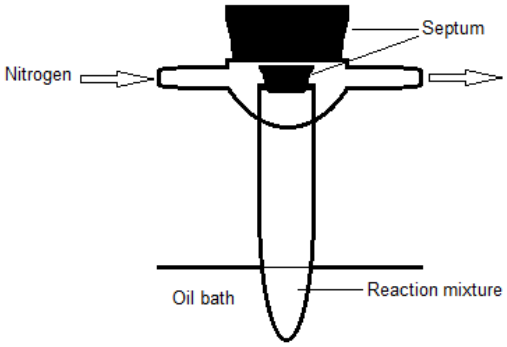

Figure S1. Reaction vessel used for the polymerization.

2. Syntheses

All reagents were purchased from ABCR, Acros Organics, Alfa Aesar, Apollo Scientific, Sigma-Aldrich or TCI chemicals and were used without further purification unless otherwise noted. Dry pyridine and dry *N*-*N*-dimethylformamide (DMF) were commercially available. THF was distilled from sodium/benzophenone. All solvents were degassed before use. *N*-*N*-bis(4-butylphenyl)-(4-vinyl)aniline (**1**),[4] *N*-(2-Ethyl-hexyl)-*N*'-(vinylphenyl)-naphthalene-1,4,5,8-dicarboxydiimide (**2**),[5] [Ru(dqp-OH)(CH_3CN)$_3$][PF_6]$_2$,[6] 4-bromophenyl-2,6-di(quinolin-8-yl)pyridine[7], **P**,[6] **D$_n$–P**,[4] and **P–A$_m$**[5] were prepared as previously described. Dqp-OH is 4-hydroxy-2,6-di(quinolin-8-yl)pyridine), PMDETA is *N,N,N′,N″,N″*-pentamethyldiethylenetriamine.

4-(4-(Triisopropylsilyl)ethinyl)phenyl-2,6-di(quinolin-8-yl)pyridine (dqp-ph-C≡C-TIPS). A flask was charged with 4-bromophenyl-2,6-di(quinolin-8-yl)pyridine (0.700 g, 1.433 mmol), $Pd(PPh_3)_4$ (0.099 g, 0.086 mmol) and copper(I) iodide (0.016 g, 0.086 mmol), sealed and placed under a nitrogen atmosphere. Then dry THF (50 mL), dry triethylamine (25 mL) and triisopropylsilylacetylene (0.6 mL, 2.674 mmol) were added via a syringe and the mixture was heated to 60 °C for 16 h until the TLC (CH_2Cl_2/MeOH 99/1, silica) showed full conversion. The reaction mixture was allowed to cool to room temperature and was filtered over Celite. The solvents were removed under reduced pressure and the residual crude product was purified by flash column chromatography (silica, eluent: CH_2Cl_2/EtOAc 90/10 followed by CH_2Cl_2/MeOH 99/1). The combined product-containing fractions were dried in vacuo to yield the product as off-white solid. (0.695 g, 85%). ^{1}H NMR (250 MHz, $CDCl_3$): δ 9.08–8.93 (m, 2H), 8.37–8.19 (m, 6H), 7.90 (d, *J* = 8.1 Hz, 2H), 7.78 (d, *J* = 7.7 Hz, 2H), 7.68 (t, *J* = 7.7 Hz, 2H), 7.60 (d, *J* = 7.7 Hz, 2H), 7.46 (dd, *J* = 8.1, 4.0 Hz, 2H), 1.15 (s, 21H). ^{13}C NMR (63 MHz, $CDCl_3$): δ 157.5, 150.5, 146.4, 146.2, 139.5, 139.4, 136.5, 132.7, 131.7, 128.8, 128.7, 127.5, 126.8, 123.9, 123.8, 121.1, 107.0, 92.1, 18.8, 11.5. MS (MALDI-ToF, DCTB) m/z: 590.39 ([C40H39N3Si+H]$^+$). HR-ESI ([C40H39N3Si+H]$^+$) m/z: calc: 590.2986, found: 590.2964, Error: 3.7 ppm.

Poly(triaryl amine) (pTARA). A glass tube equipped with a septum and an external overhead flushing with nitrogen was used for the polymerization (Figure S1). The reaction vessel was charged with **1** (0.940 g, 2.451 mmol), *N*-(*tert*-butyl)-*O*-(1-(4-(chloromethyl)phenyl)ethyl)-*N*-(2-methyl-1-phenylpropyl)hydroxylamine (CMSt-TIPNO) (0.046 g, 0.123 mmol) and anisole (2.4 mL).The mixture was purged with nitrogen for 20 min and placed in a pre-heated oil bath (120 °C). After 23 h the reaction mixture was diluted with CH_2Cl_2 and precipitated in cold MeOH. Subsequently, unreacted monomer was removed by preparative SEC (Bio-Beads S-X1, CH_2Cl_2). The polymer was obtained as yellow solid after precipitation in MeOH. Yield: 0.465 g. SEC ($CHCl_3$/2-propanol/NEt_3 94/2/4, PS calibration): M_n = 4,600 g/mol, Đ = 1.06. ^{1}H NMR (300 MHz, $CDCl_3$): δ 7.56 – 7.06 (br), 7.06 – 6.13 (br), 4.60 – 4.21 (br), 2.72 – 2.65 (br), 2.65 – 1.78 (br), 1.78 – 1.42 (br). 1.42 – 1.18 (br), 1.18 – 0.74 (br), 0.74 – 0.11 (br).

Poly(naphthalene diimide) (pNDI, Cl-decorated). A glass tube equipped with a septum and an external overhead flushing with nitrogen was used for the polymerization (Figure S1). The reaction vessel was charged with **2** (0.500 g, 1.040 mmol), *N*-(*tert*-butyl)-*O*-(1-(4-(chloromethyl)phenyl)ethyl)-*N*-(2-methyl-1-phenylpropyl)hydroxylamine (CMSt-TIPNO) (0.019 g, 0.052 mmol) and anisole (4.0 mL).The mixture was purged with nitrogen for 20 min and placed in a pre-heated oil bath (120 °C). After 17 h the reaction mixture was diluted with CH_2Cl_2 and precipitated in cold MeOH. Subsequently, unreacted monomer was removed by preparative SEC (Bio-Beads S-X1, CH_2Cl_2). The polymer was obtained as yellow solid after precipitation in MeOH. Yield: 0.400 g. SEC ($CHCl_3$/2-propanol/NEt_3 94/2/4, PS calibration): M_n = 6,400 g/mol, Đ = 1.11. ^{1}H NMR (300 MHz, $CDCl_3$): δ 9.04 – 7.98 (br), 7.78 – 6.67 (br), 4.72 – 4.42 (br), 4.34 – 3.60 (br), 2.91 – 1.72 (br), 1.52 – 1.04 (br). 1.04 – 0.45 (br).

Poly(naphthalene diimide) (pNDI, azide-decorated). *Safety advice: Sodium azide is very toxic, personal protection precautions should be taken. Heavy metal azides are explosive. Do not use metal spatula.* A glass vial was charged with **pNDI (Cl-decorated)** (0.150 g, 0.024 mmol, 1 eq.) and sodium azide (0.005 g, 0.071 mmol, 3 eq.), capped and placed under a nitrogen atmosphere. Dry DMF (4.5 mL) was added and the reaction mixture was immersed in an oil bath at 60 °C at which the polymer dissolved. After 48 h CH_2Cl_2 and water were added to the formed suspension and the layers were separated. The aqueous layer was extracted two times with CH_2Cl_2. The combined organic layers were three times washed with brine and dried over Na_2SO_4. After removal of the solvent under reduced pressure, a yellow solid was obtained. Yield: 0.135 g. SEC ($CHCl_3$/2-propanol/NEt_3 94/2/4, PS calibration): M_n = 6,300 g/mol, Đ = 1.08. ^{1}H NMR (300 MHz, $CDCl_3$): δ 9.04 – 7.98 (br), 7.78 – 6.66 (br), 4.56 – 4.22 (br), 4.23 – 3.60 (br), 2.83 – 1.65 (br), 1.51 – 1.05 (br), 1.05 – 0.45 (br).
Note: The quantitative substitution was verified by a shift of the methylene proton resonance of **pNDI** (azide-decorated). *(from 4.6 ppm to 4.3 ppm).*

[Ru(dqp-OH)(dqp-ph-C≡C-TIPS)][PF_6]$_2$. A flask was charged with [Ru(dqp-OH)(CH_3CN)$_3$][PF_6]$_2$ (0.450 g, 0.521 mmol), dqp-ph-C≡C-TIPS (0.307 g, 0.521 mmol) and dry DMF (10 mL) under nitrogen. Subsequently the reaction mixture was heated to 140 °C for 48 h. After cooling to room temperature the solution was precipitated in an aqueous NH_4PF_6 solution, filtered and re-dissolved in CH_3CN. The crude product was purified by column chromatography on silica using a mixture of $CH_3CN/H_2O/KNO_{3(aq)}$ (40/4/1) as eluent. Afterwards on anion exchange was performed by precipitation in an aqueous NH_4PF_6 solution. Finally, diffusion controlled crystallization (diethyl ether into acetonitrile solution) gave the desired complex as red solid (0.350 g, 51%). ^{1}H NMR (600 MHz, CD_3CN): δ 9.15 (br, OH), 8.13 (m, 4H), 8.06 (m, 6H), 7.93 (d, *J* = 8.5 Hz, 2H), 7.86 (dd, *J* = 1.1 Hz, 7.5 Hz, 2H), 7.71 (dd, *J* = 1.1 Hz, 7.3 Hz, 2H), 7.67 (m, 6H), 7.45 (m, 4H), 7.37 (s, 2H), 7.07 (m, 4H), 1.16 (m, 21H). ^{13}C NMR (150 MHz, CD_3CN): δ 166.2, 159.6, 159.5, 158.5, 158.2, 149.1, 147.6 (2×), 138.4, 138.3, 137.1, 134.3, 133.7, 133.6, 132.9, 132.6, 131.5 (2×), 128.6, 127.7, 127.6, 127.5, 126.1, 125.9, 122.9, 116.7, 107.2, 94.2,

18.9, 12.0. HR-ESI-ToF-MS: $[C_{63}H_{54}N_6ORuSi]^{2+}$ m/z: calculated: 520.1580, found: 520.1599, error: 1.9 ppm.

[Ru(dqp-O-pTARA)(dqp-ph-C≡C-TIPS)][PF_6]$_2$. A vial was charged with **pTARA** (0.400 g, 0.087 mmol) and anisole (1.5 mL). Then [Ru(dqp-OH)(dqp-ph-C≡C-TIPS)][PF_6]$_2$ (0.231 g, 0.174 mmol), KI (0.029 g, 0.174 mmol), K_2CO_3 (0.024 g, 0.174 mmol) and DMF (1.5 mL) were added. Subsequently, the vial was capped and immersed in a preheated oil bath at 60 °C. The reaction progress was monitored by UV/vis SEC and TLC (aluminium oxide, CH_2Cl_2/MeOH 95/5). After 89 h no further conversion was detected and the reaction mixture was cooled to room temperature. An aqueous solution of NH_4PF_6 was added and the suspension was extracted with CH_2Cl_2 (3 ×). The organic extracts were dried over Na_2SO_4 and concentrated under reduced pressure. The desired dyad was isolated by preparative SEC (Toyopearl HW-55F, CH_2Cl_2/MeOH 95/5) as red solid (0.250 g, 48%). ^{1}H NMR (600 MHz, CD_2Cl_2): δ 8.17 (br, Ru), 8.10 (br, Ru), 7.96 (br, Ru), 7.73 (br, Ru), 7.60 (br, Ru), 7.53 (br, Ru), 7.39 (br, Ru), 7.26 (br, Ru), 7.05 – 5.81 (br, p1$_{15}$), 5.46 (br, linker), 5.24 (br, linker), 2.64 – 2.34 (br, (br, p1$_{15}$), 2.34 – 1.85 (br, p1$_{15}$), 1.85 – 1.43 (br, p1$_{15}$). 1.43 – 1.22 (br, p1$_{15}$), 1.22 – 1.15 (br, TIPS), 1.00 – 0.72 (br, p1$_{15}$).

[Ru(dqp-O-pTARA)(dqp-ph-C≡C-H)][PF_6]$_2$. A vial was charged with [Ru(dqp-O-pTARA)(dqp-ph-C≡C-TIPS)][PF_6]$_2$ (0.230 g, 0.038 mmol) under nitrogen. Then dry THF (5.0 mL) was added and the resulting solution was cooled with an ice bath. Subsequently, a solution of (*n*-Bu_4)NF (0.040 g, 0.143 mmol) in THF (0.265 mL) was added and the mixture was stirred for 0.5 h at 0 °C. Afterwards, water was added and the solution was extracted with CH_2Cl_2. The organic extracts were dried over Na_2SO_4 and concentrated under reduced pressure. The red solid was washed with CH_3CN and was dried (0.230 g, 100%). ^{1}H NMR (300 MHz, CD_2Cl_2): δ 8.04 (br, Ru), 7.99 (br, Ru), 7.79 (br, Ru), 7.65 (br, Ru), 7.51 (br, Ru), 7.33 (br, Ru), 7.14 (br, Ru), 7.04 – 6.30 (br, p1$_{15}$), 5.14 (br, linker), 2.63 – 2.28 (br, p1$_{15}$), 2.25 – 1.62 (br, p1$_{15}$), 1.62 – 1.39 (br, p1$_{15}$). 1.39 – 1.18 (br, p1$_{15}$), 0.97 – 0.74 (br, p1$_{15}$).

[Ru(dqp-O-pTARA)(dqp-ph-trz-pNDI)][PF_6]$_2$ (D_n–P–A_m). A vial was charged with [Ru(dqp-O-pTARA)(dqp-ph-C≡C-H)][PF_6]$_2$ (0.014 g, 0.003 mmol, 1 eq.) and pNDI (azide-decorated) (0.030 g, 0.005 mmol, 2 eq.) under nitrogen. Then dry DMF (1.0 mL), solution of CuBr (0.001 g, 0.010 mmol, 4 eq.) in DMF (0.2 mL) and PMDETA (0.24 M in DMF, 0.04 mL, 4 eq.) were added. The mixture was heated to 80 °C for 96 h. The mixture was precipitated in aqueous NH_4PF_6 and the red solid was extracted with CH_2Cl_2. After drying over Na_2SO_4, the desired triad **D_n–P–A_m** was purified by preparative size-exclusion chromatography (Toyopearl HW-55F, CH_2Cl_2/MeOH 95/5, two runs) and was isolated as light red solid (0.017 g, 58%). ^{1}H NMR (300 MHz, CD_2Cl_2): δ 8.84 − 8.17 (br, p2$_{17}$), 8.08 (br, Ru), 7.91 (br, Ru), 7.68 (br, Ru), 7.64 − 7.04 (br, Ru + p2$_{17}$), 7.04 – 6.29 (br, p1$_{15}$), 5.57 (br, linker), 5.20 (br, linker), 4.32 − 3.58 (br, p2$_{17}$), 2.96 – 2.29 (br, p1$_{15}$), 2.29 – 1.59 (br, p1$_{15}$ + p2$_{17}$), 1.59 – 1.44 (br, p1$_{15}$). 1.39 – 1.04 (br, p1$_{15}$ + p2$_{17}$), 1.04 – 0.46 (br, p1$_{15}$ + p2$_{17}$).

3. NMR spectroscopy

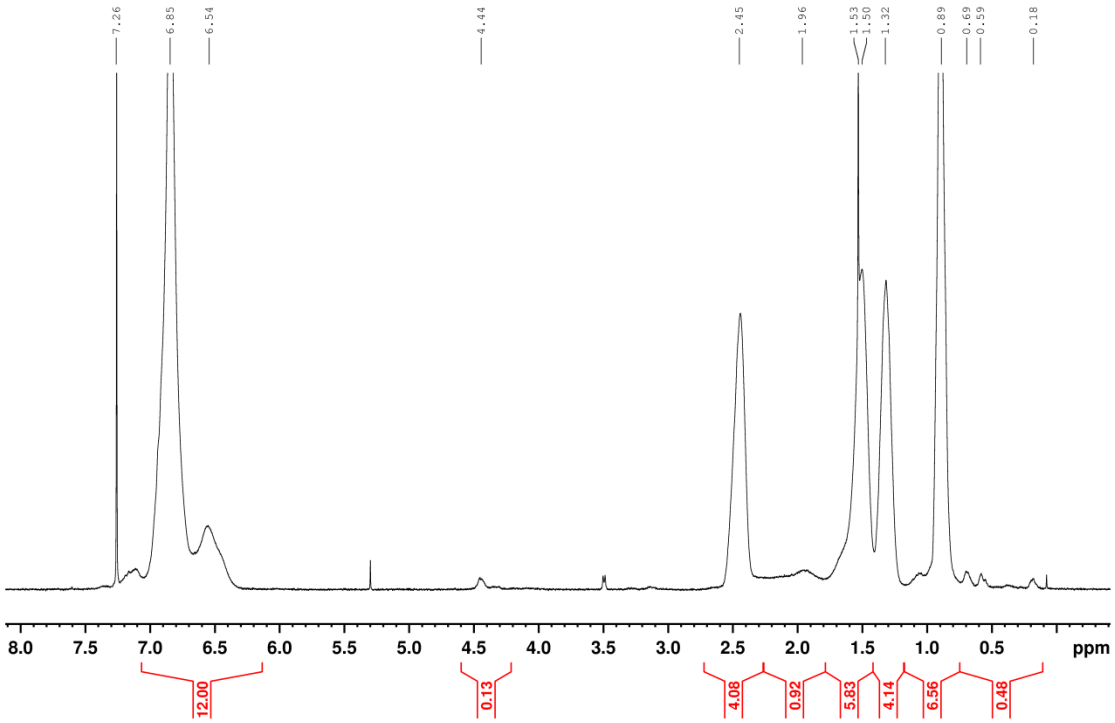

Figure S2. ^{1}H NMR spectrum (300 MHz, $CDCl_3$) of **pTARA**.

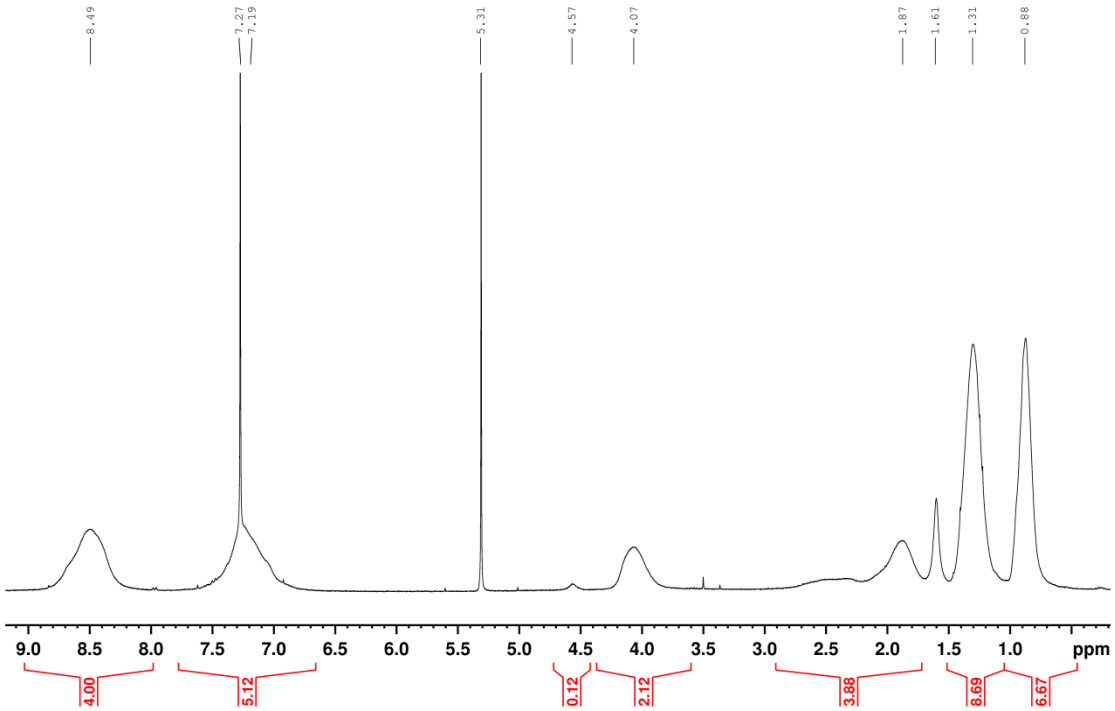

Figure S3. ^{1}H NMR spectrum (300 MHz, $CDCl_3$) of **pNDI (Cl-decorated)**. Note the chloromethyl group at 4.57 ppm.

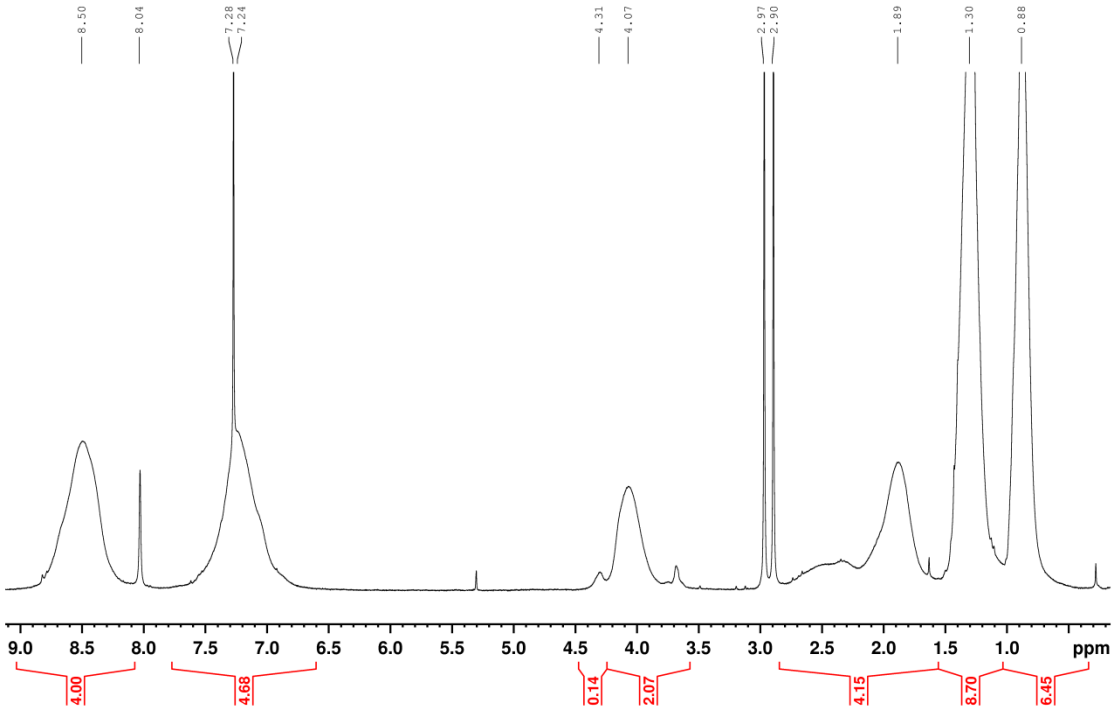

Figure S4. ^{1}H NMR spectrum (300 MHz, $CDCl_3$) of **pNDI** (azide-decorated).

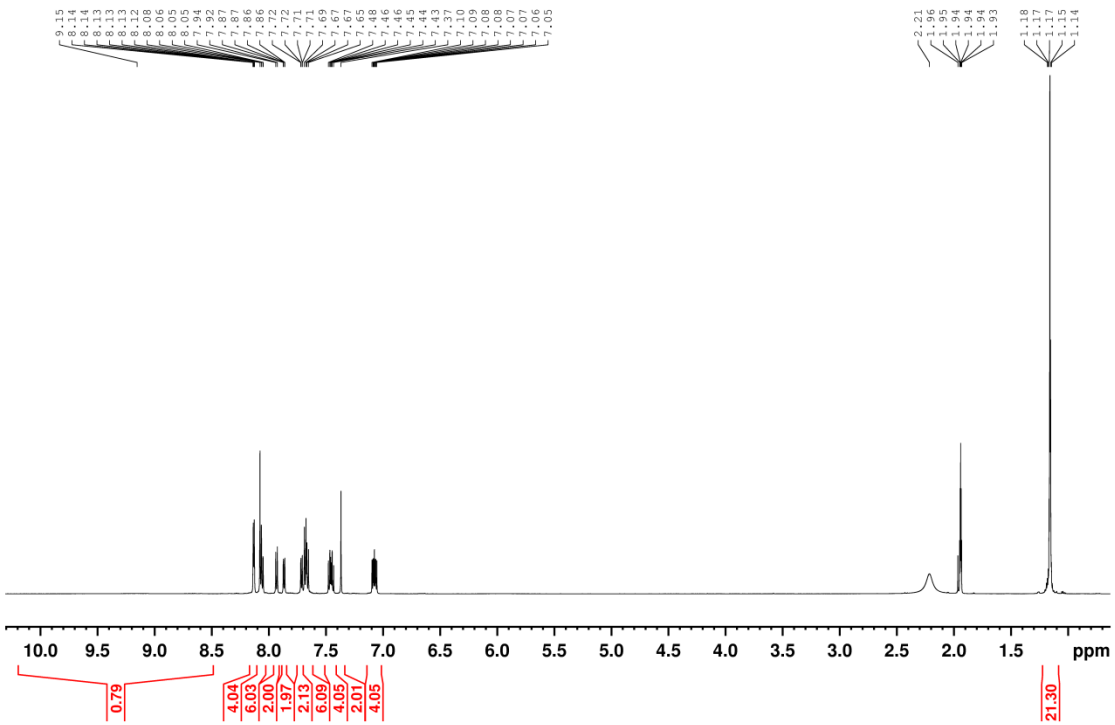

Figure S5. ^{1}H NMR spectrum (600 MHz, CD_3CN) of [Ru(dqp-OH)(dqp-ph-C≡C-TIPS)][PF_6]$_2$.

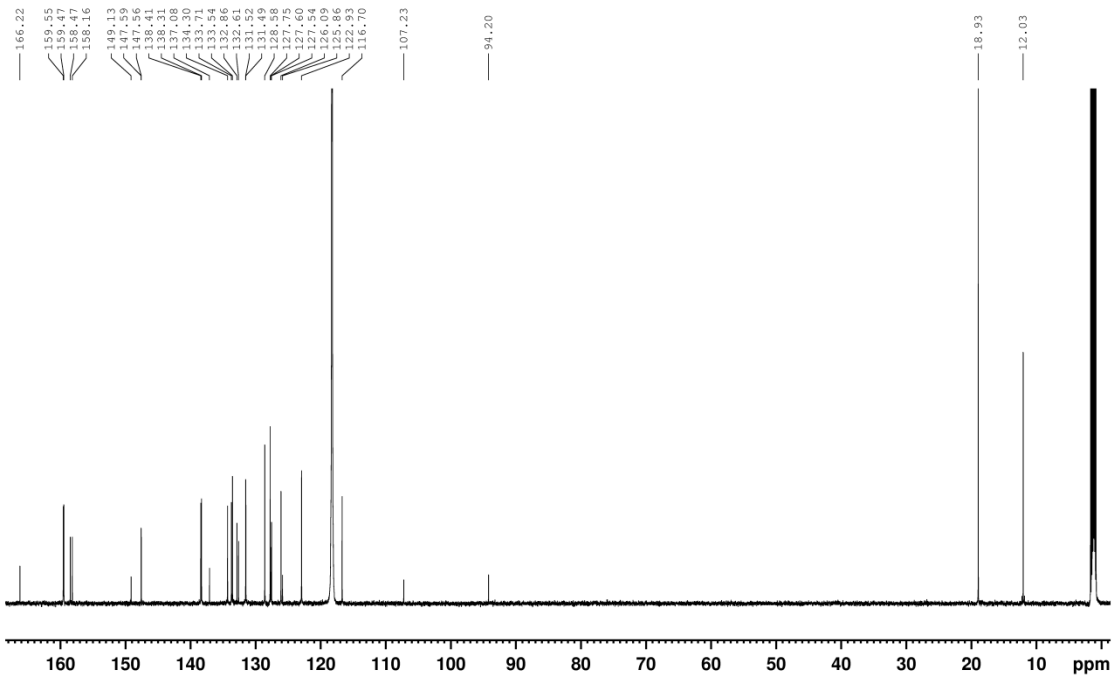

Figure S6. ^{13}C NMR spectrum (150 MHz, CD_3CN) of $[Ru(dqp\text{-}OH)(dqp\text{-}ph\text{-}C{\equiv}C\text{-}TIPS)][PF_6]_2$.

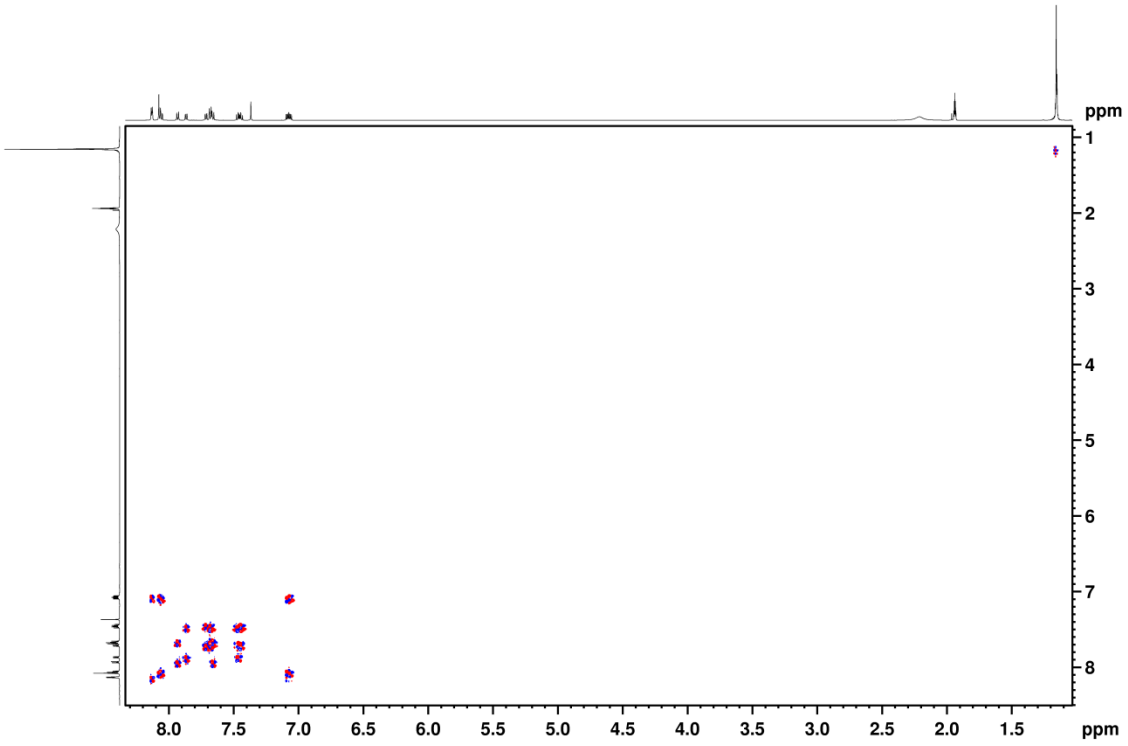

Figure S7. H,H COSY spectrum of $[Ru(dqp\text{-}OH)(dqp\text{-}ph\text{-}C{\equiv}C\text{-}TIPS)][PF_6]_2$.

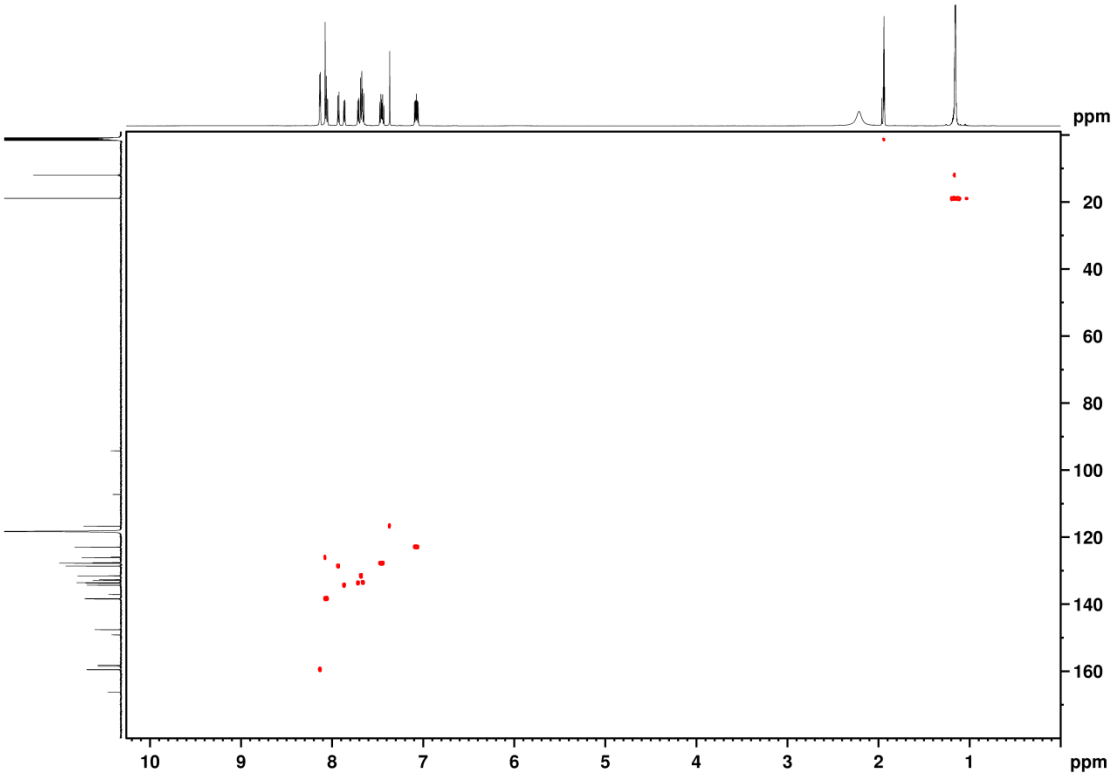

Figure S8. HSQC spectrum of [Ru(dqp-OH)(dqp-ph-C≡C-TIPS)][PF_6]$_2$.

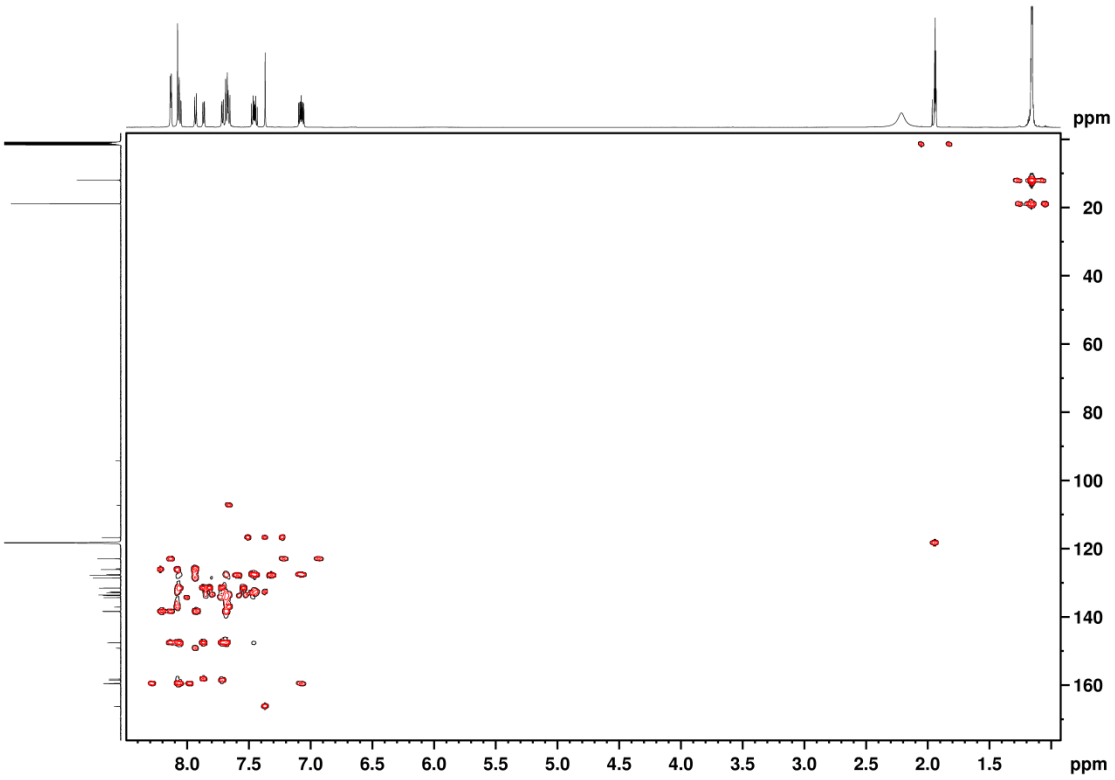

Figure S9. HMBC spectrum of [Ru(dqp-OH)(dqp-ph-C≡C-TIPS)][PF_6]$_2$.

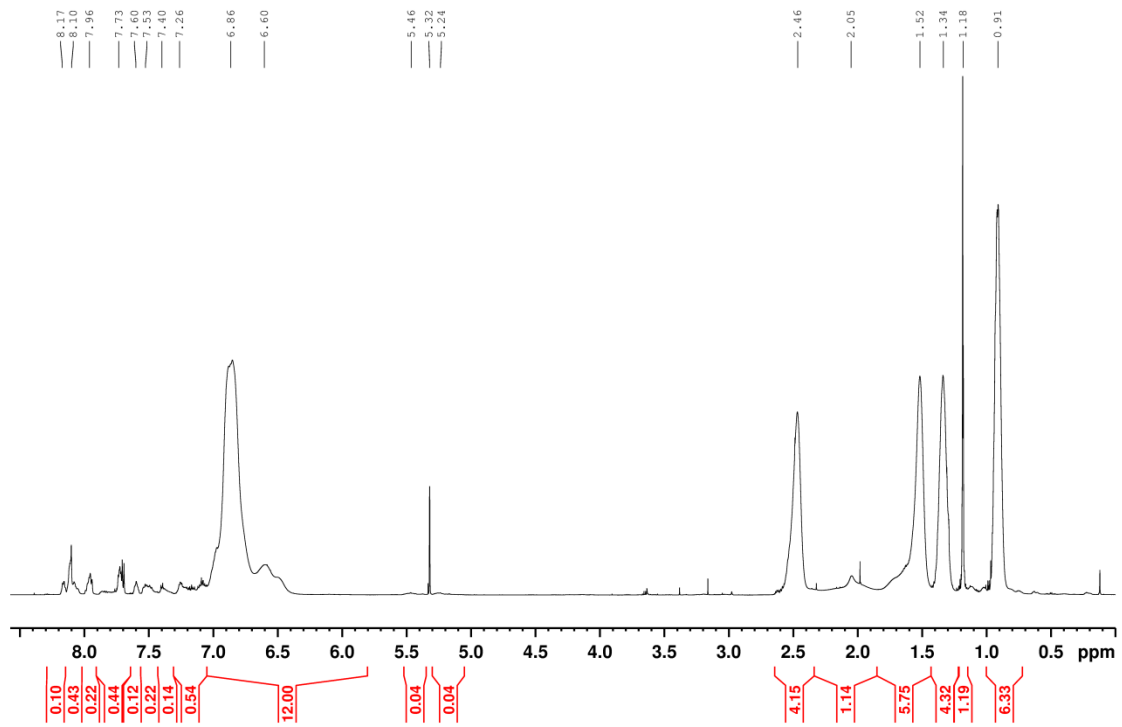

Figure S10. ^{1}H NMR spectrum (300 MHz, CD_2Cl_2) of [Ru(dqp-O-pTARA)(dqp-ph-C≡C-TIPS)][PF_6]$_2$. Note the downfield shift of the methylene group upon linkage (from 4.57 in Figure S3) to 5.5 ppm.

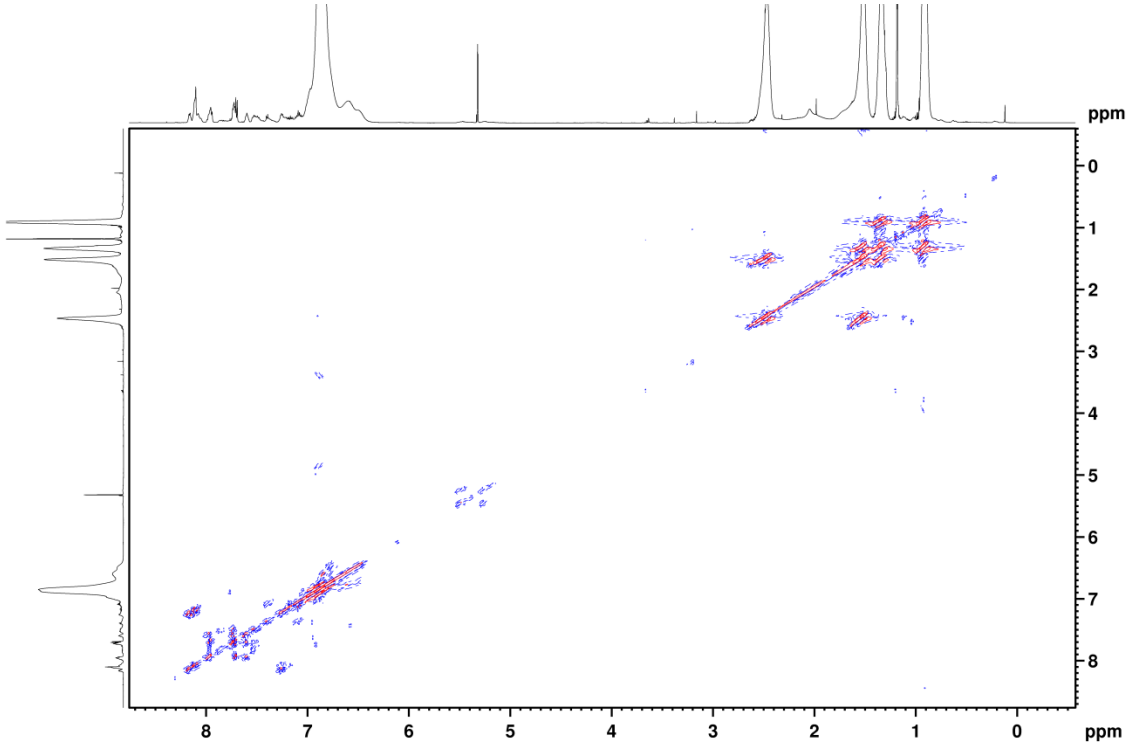

Figure S11. H,H COSY spectrum of [Ru(dqp-O-pTARA)(dqp-ph-C≡C-TIPS)][PF_6]$_2$.

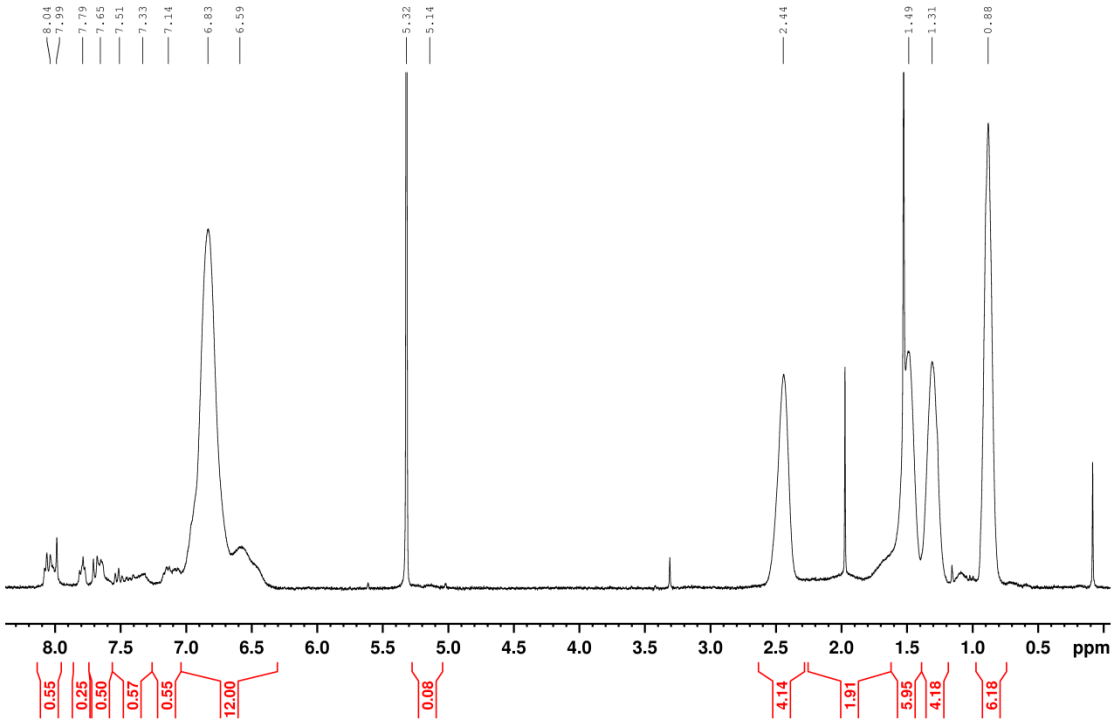

Figure S12. ^{1}H NMR spectrum (300 MHz, CD_2Cl_2) of [Ru(dqp-O-pTARA)(dqp-ph-C≡CH)][PF_6]$_2$.

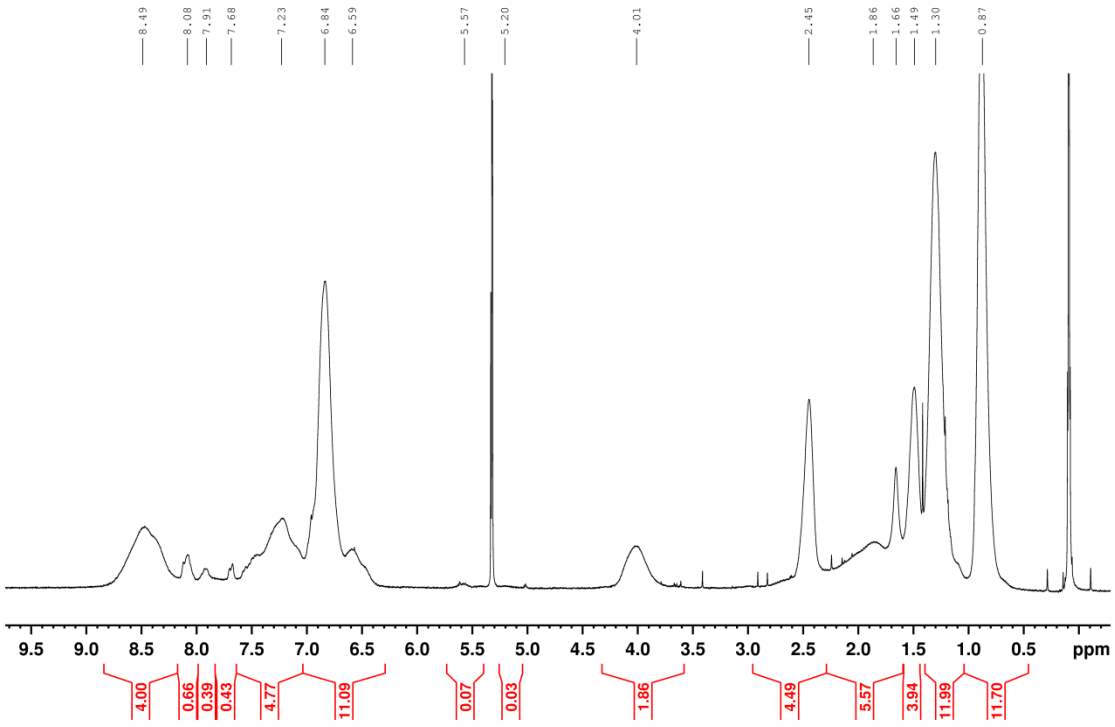

Figure S13. ^{1}H NMR spectrum (300 MHz, CD_2Cl_2) of [Ru(dqp-O-pTARA)(dqp-ph-trz-pNDI)][PF_6]$_2$ (D_n–P–A_m).

4. Mass spectrometry

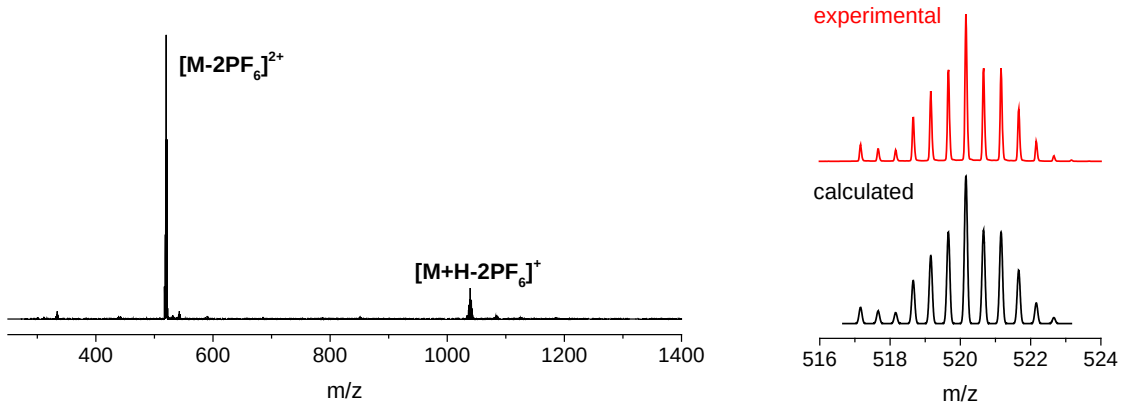

Figure S14. ESI TOF MS data of [Ru(dqp-OH)(dqp-ph-C≡C-TIPS)][PF_6]$_2$ and (right) comparison of measured and calculated isotope pattern.

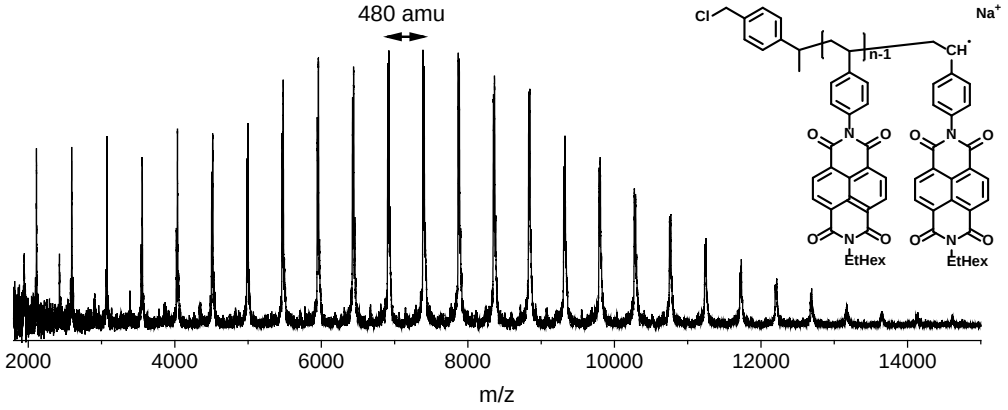

Figure S15. MALDI TOF mass spectrum of **pNDI (Cl-decorated)** (matrix: HABA + NaTFA) with proposed structure of the main series.

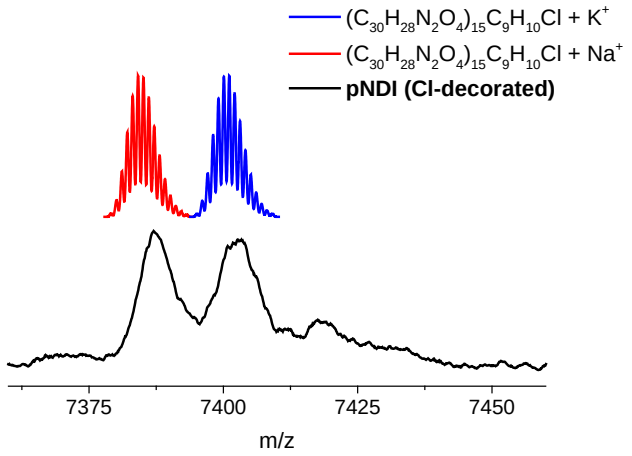

Figure S16. Theoretical (top) isotopic patterns to fit the experimental (bottom) data of the signal corresponding to a DP = 15 (matrix: HABA + NaTFA).

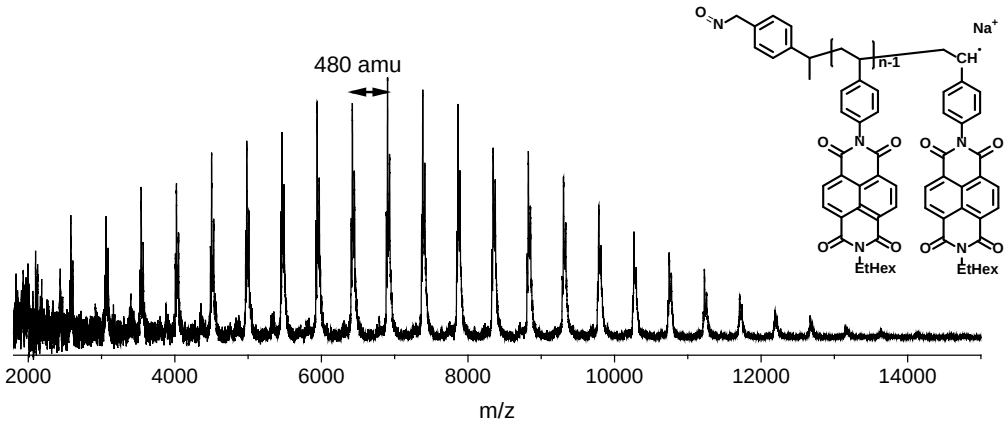

Figure S17. MALDI TOF mass spectrum of **pNDI (azide-decorated)** (matrix: HABA + NaTFA) with proposed structure of the main series.

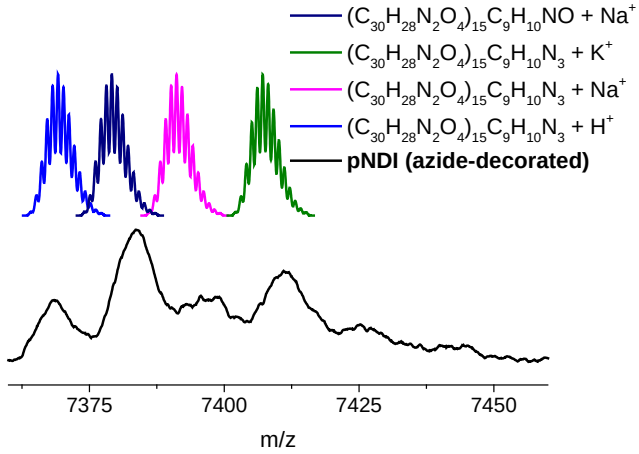

Figure S18. Theoretical (top) isotopic patterns to fit the experimental (bottom) data of the signal corresponding to a DP = 15 (matrix: HABA + NaTFA).

5. Size-exclusion chromatography

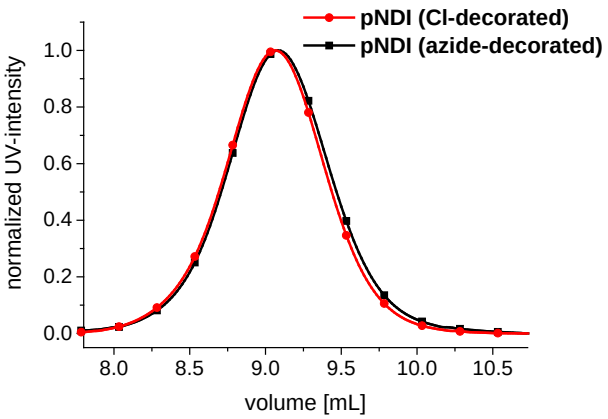

Figure S19. SEC elugrams of **pNDI** (Cl-decorated and azide-decorated) showing the absence of degradation during the functionalization (UV: 340 nm detection wavelength, $CHCl_3$, *iso*-propanol, triethylamine 94/2/4).

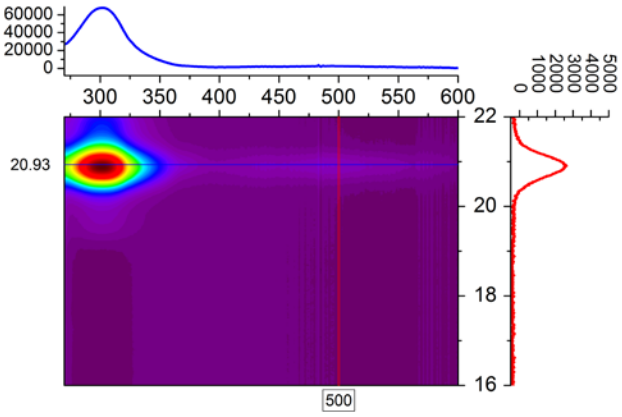

Figure S20. 3D SEC data (wavelength vs elution time, DMAc + 0.08% NH_4PF_6) of [Ru(dqp-O-pTARA)(dqp-ph-C≡C-TIPS)][PF_6]$_2$ (**D_n–P**) with projections: (top) UV trace at 20.03 mL; (right) chromatogram at 500 nm in a.u..

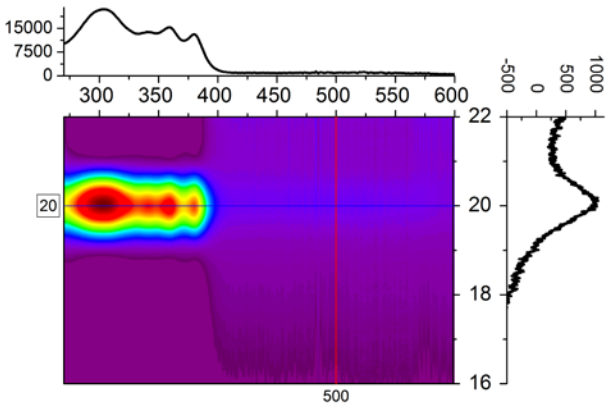

Figure S21. 3D SEC data (wavelength vs elution time, DMAc + 0.08% NH_4PF_6) of [Ru(dqp-O-pTARA)(dqp-ph-trz-pNDI)][PF_6]$_2$ (**D_n–P–A_m**) with projections: (top) UV trace at 20.03 mL; (right) chromatogram at 500 nm in a.u..

6. Steady state optical data

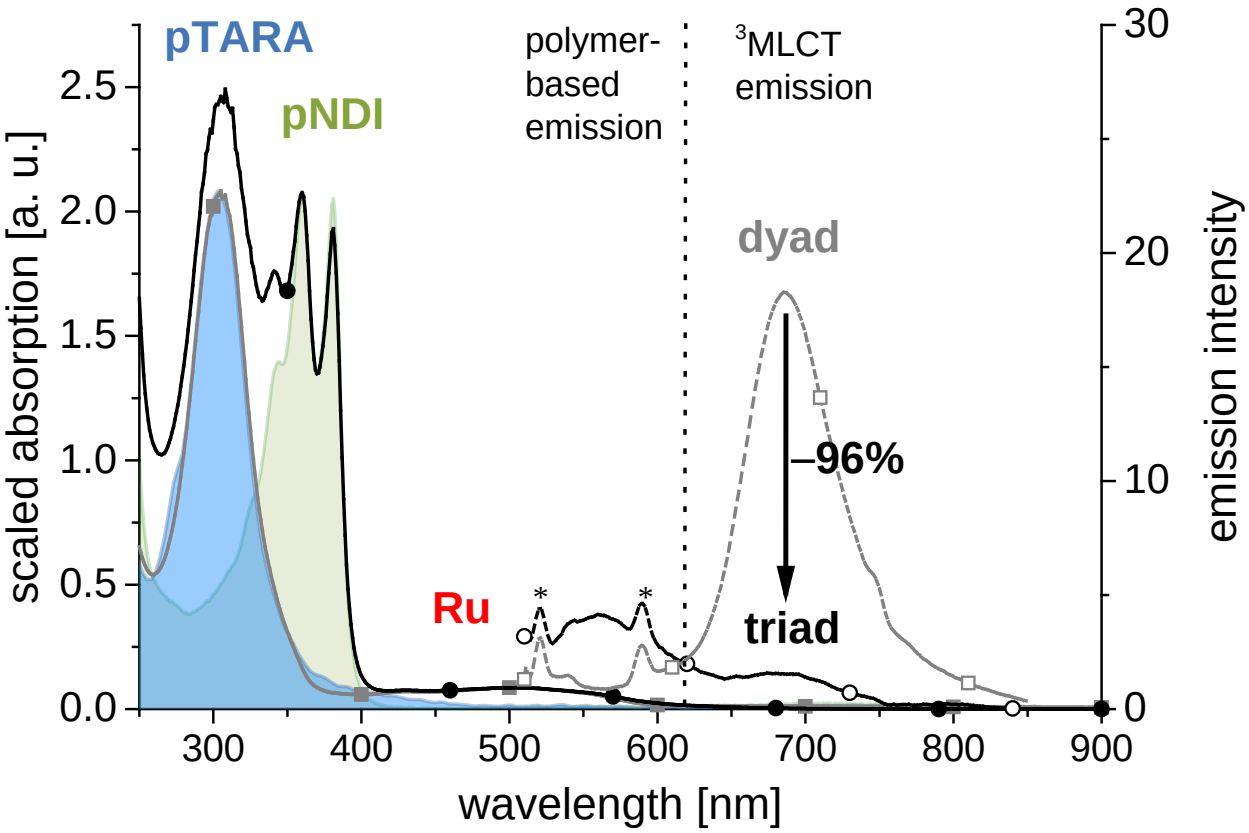

Figure S22. Enlarged version: Absorption spectra (left axis) of the triad (black curve, circles), including its precursor dyad (grey curve, rectangles) and the polymeric building blocks **pTARA** (blue-shaded area) and **pNDI** (green-shaded area). Note the absorption band of the single Ru photosensitizer unit (400–600 nm). Steady-state emission spectra (right axis) of the precursor dyad (grey dashed line, rectangles) and the triad (black dashed line, circles). Note polymer-based emission (<650 nm) and the ^{3}MLCT emission (around 700 nm), the latter one quenched by 96% comparing donor dyad (**D_n–P**) and full triad (**D_n–P–A_m**) (subtracting residual polymer-based emission). All measurements were performed in aerated DCM solution, asterisk (*) denotes Raman artefacts**.**

7. Spectroelectrochemical data

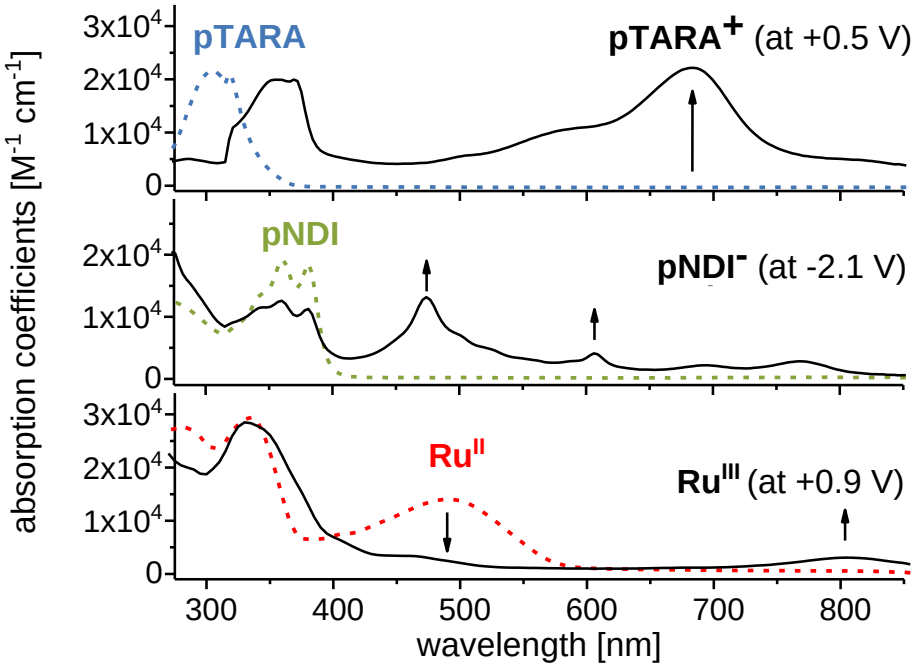

Figure S23. Spectro-electrochemical data (in 0.1 M $^{n}Bu_4NPF_6$ in CH_2Cl_2, potentials *vs.* $Fc^{+/0}$) of the **pTARA** block (top), the **pNDI** block (middle), and the reference complex $[Ru(dqp)_2]^{2+}$ (bottom). Spectroelectrochemical data taken from refs. [5, 8]

8. Time-resolved data

8.1. Emission data

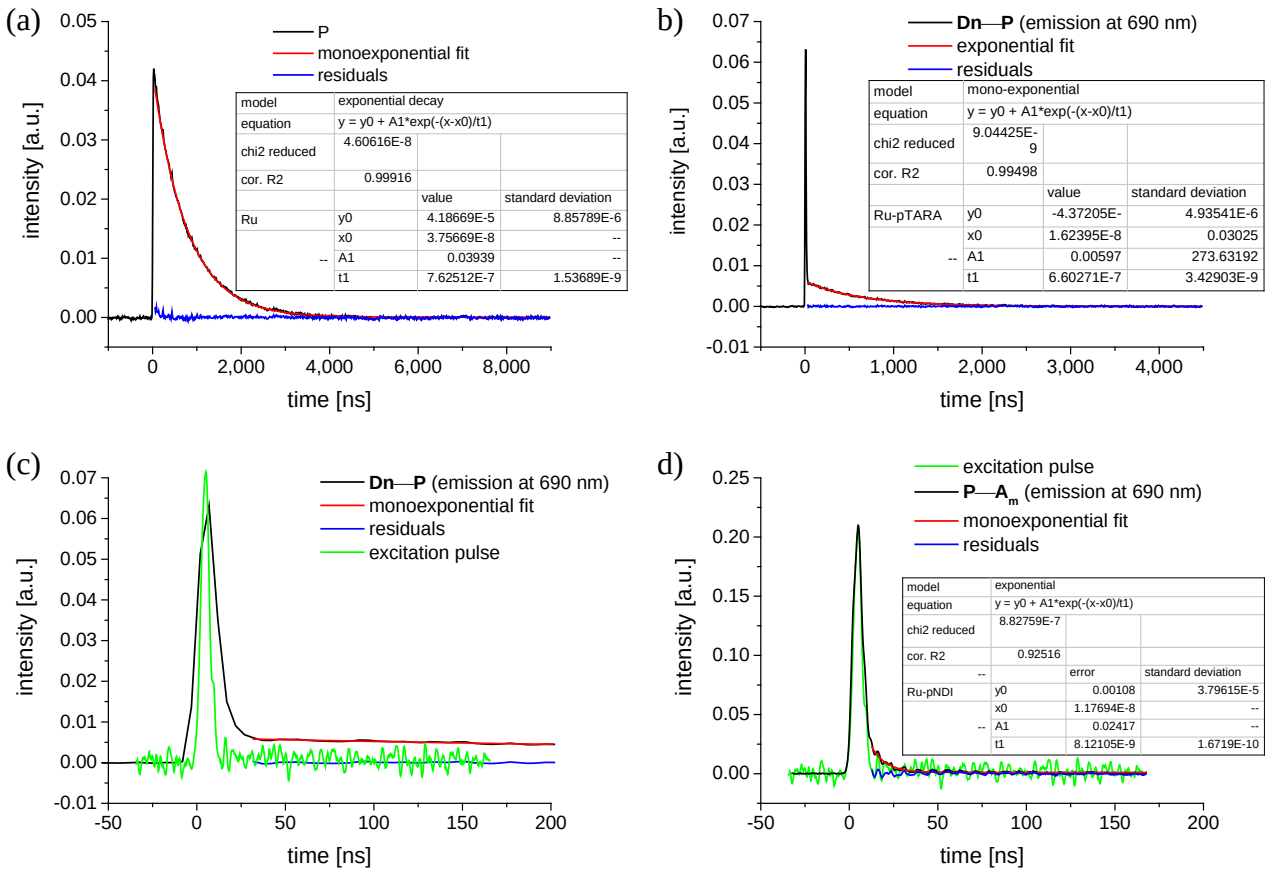

Figure S24. Emission data and respective fits for the reference systems: (a) Photosensitizer (**P**), (b) donor dyad (**D_n–P**) with zoom of the pulse region (c), and (d) acceptor dyad (**P–A_m**) including pulse (green). Excitation pulse width (approximately 10 ns) determined from Raman scatter of a pure DCM sample.

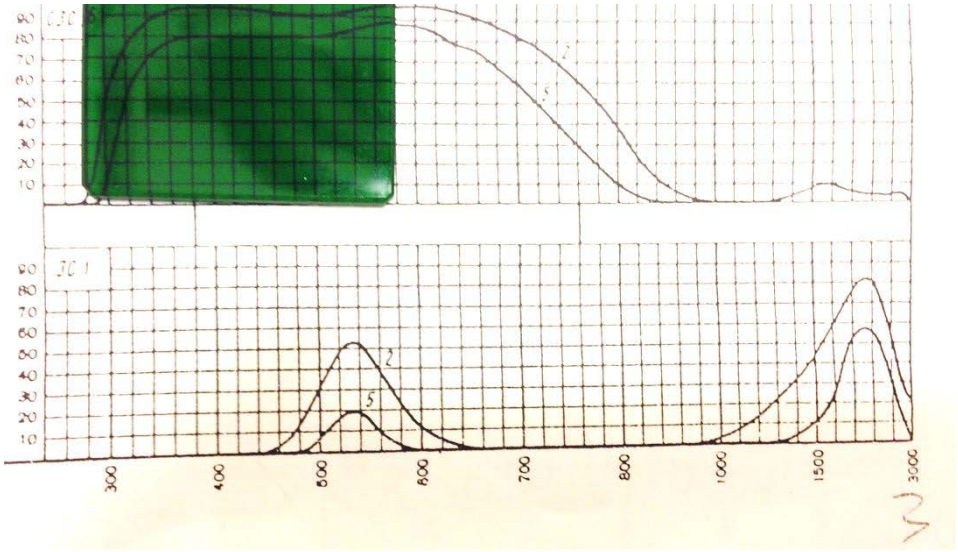

Figure S25. Transmission properties of band pass filter (3C1) used in TCSPC measurements (λ_{max} = 540 nm with FWHM ca. 100 nm. Note that blocked transmission above 650 nm, which is typical for the ^{3}MLCT emission.

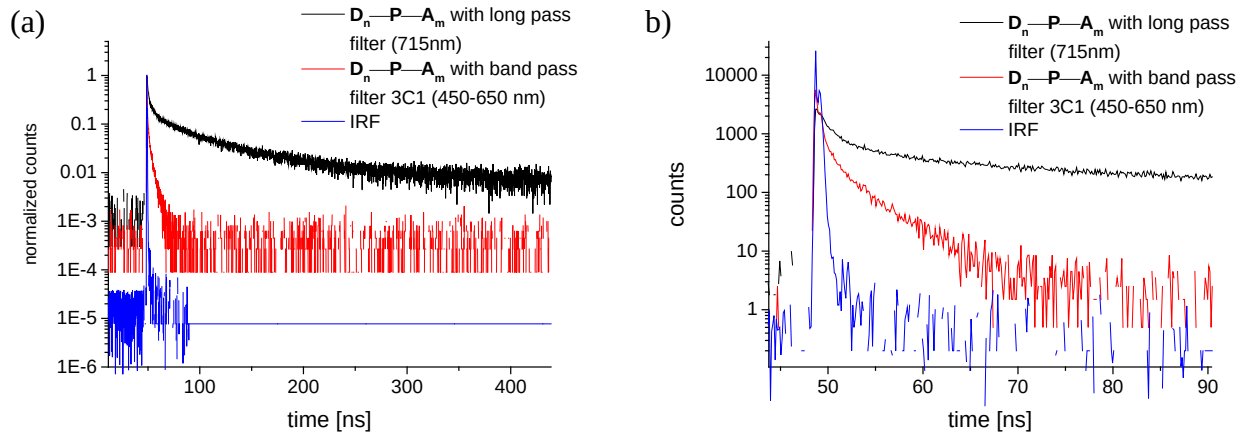

Figure S26. Normalized time-correlated single photon counting data of **D_n–P–A_m** (a) and expansion of pulse region (b). Instrument response function (IRF, blue, ca 1.3 ns), with long pass filter (>715 nm, black) and with band pass filter (3C1, 450-650 nm, red). See Figure S25 for transmission characteristics of 3C1 filter.

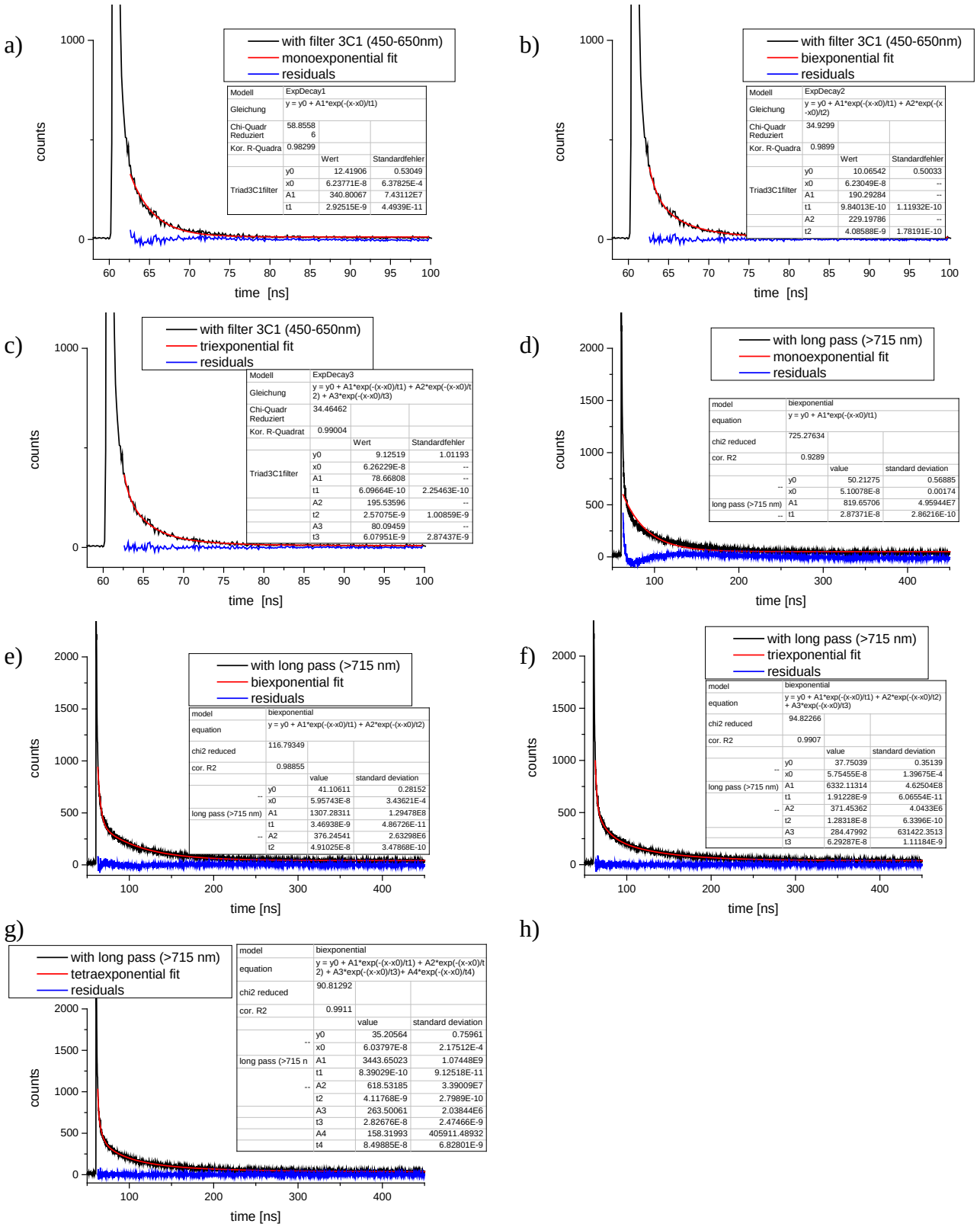

Figure S27. TCSPC data and fits of **D_n–P–A_m** using the band pass filter 3C1 (450–650 nm, a-c), and the long pass filter (>715 nm, d-g) applying multiexponential fit curves: (a,d) Monoexponential, (b, e) biexponential, (c,f) triexponential and (g) tetraexponential decay.

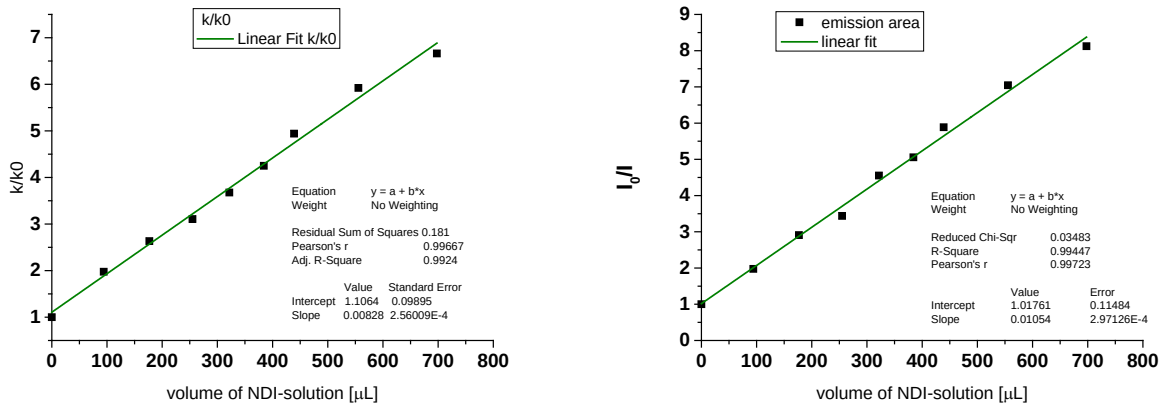

Figure S28. Stern-Vollmer analysis for initial electron transfer between Ru unit and NDI units using the D_n-Ru dyad: Bimolecular quenching confirms dynamic quenching mechanism for non-linked systems.

Table S1. Tabulated fit parameters for TCSPC data of **D_n–P–A_m**.

	450-650 nm (3C1)			>715 nm (long pass)			
	monoexponential	biexponential	triexponential	monoexponential	biexponential	triexponential	tetraexponential
Component1	2.92 ± 0.01 ns (100%)	0.98 ± 0.11 ns (45%)	0.61 ± 0.23 ns (22%)	28.73 ± 0.28 ns (100%)	3.47 ± 0.05 ns (78%)	1.91 ± 0.06 ns (91%)	0.83 ± 0.09 ns (77%)
Component2	-	4.08 ± 0.18 ns (55%)	2.57 ± 1.01 ns (55%)	-	49.1 ± 0.34 ns (22%)	12.8 ± 0.64 ns (5%)	4.11 ± 0.28 ns (14%)
Component3	-	-	6.08 ± 2.86 ns (23%)	-	-	62.9 ± 1.11 ns (4%)	28.3 ± 2.5 ns (6%)
Component 4							85.0 ± 6.8 ns (4%)
χ^2-reduced	58.856	34.930	34.465	725.28	116.79	94.823	90.813
Correlated R^2	0.9830	0.9899	0.9900	0.9289	0.9886	0.9907	0.9911

8.2. Transient absorption data

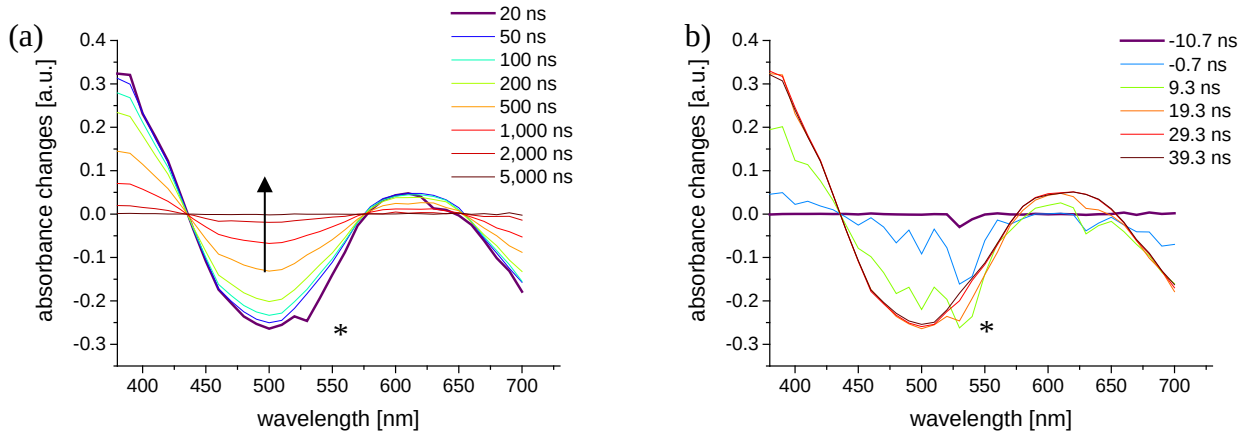

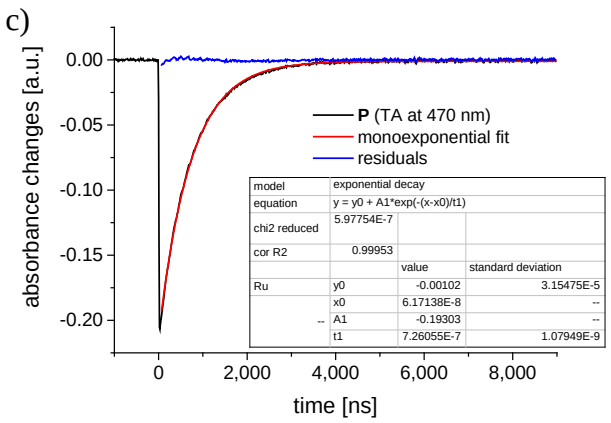

Figure S29. Transient absorption data of **P**: (a) Spectral recovery at selected times with zoom of pulse region (b). Note the isosbestic points around 435 and 575 nm. Asterisk denotes excitation pulse artefacts due to Rayleigh scatter. (c) Decay profile with fit at 470 nm.

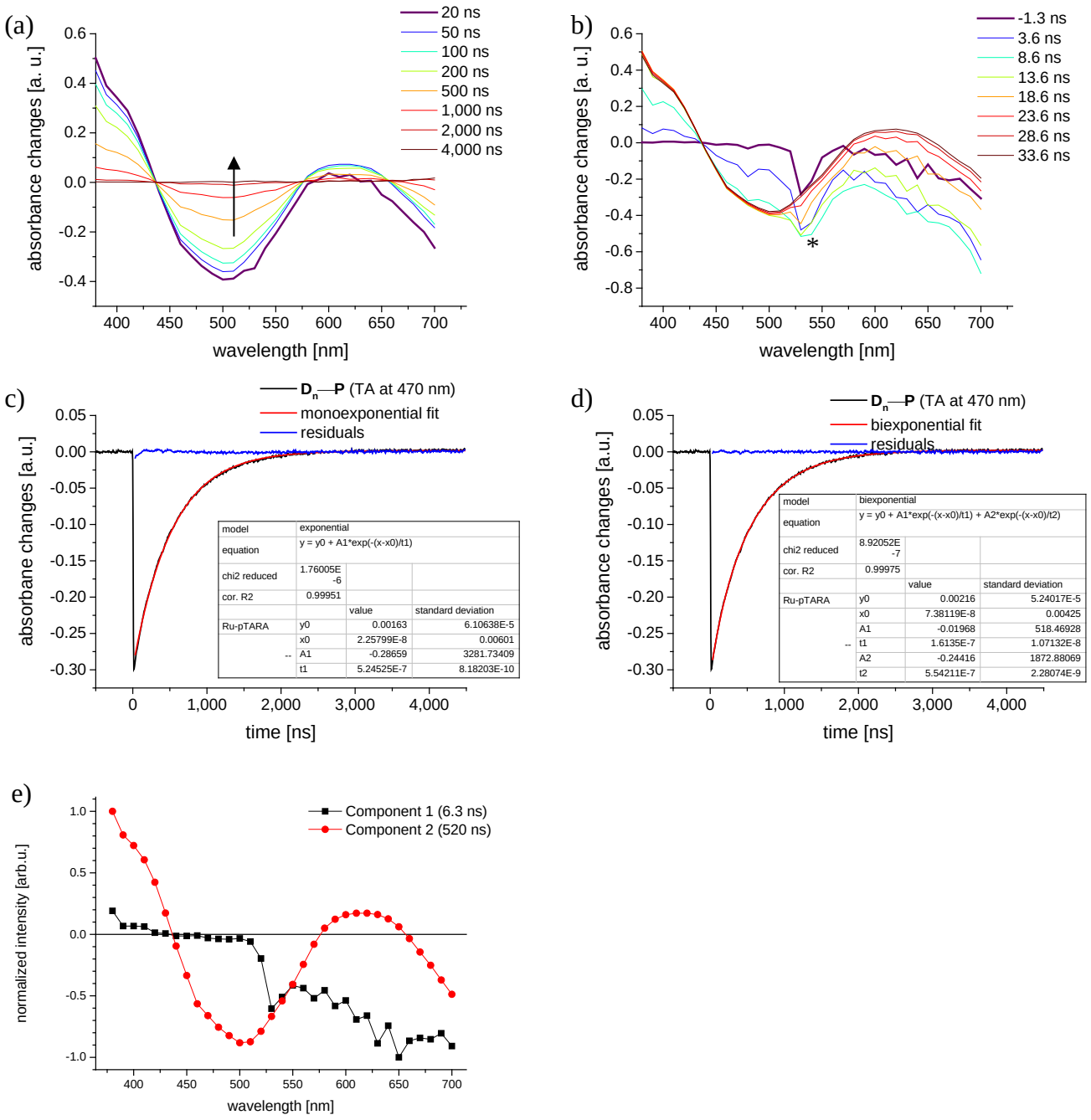

Figure S30. Transient absorption data of **D_n–P**: (a) Spectral recovery at selected times with zoom of pulse region (b). Note the preserved isosbestic point around 435 nm but clear deviation at 575 nm with respect to Ru (Figure S29), as well as weaker TA signals between 575 and 650 nm assigned to additional polymer-based emission (see text). Asterisk denotes excitation pulse artefacts including Rayleigh scatter. (c) Decay profile with fit at 470 nm including biexponential decay (d). Global fit (>= 18.6 ns) with biexponential kinetics with corresponding amplitudes (scaled for comparison). Component 1 (black curve) shows similar spectral signatures as polymer-based emission from steady state data with comparable lifetimes (6.3 ns) as observed in TCSPC with band pass filter (Figure S27), while component 2 (red curve) resembles **P** in terms for its spectrum and lifetime (520 ns, Figure S29).

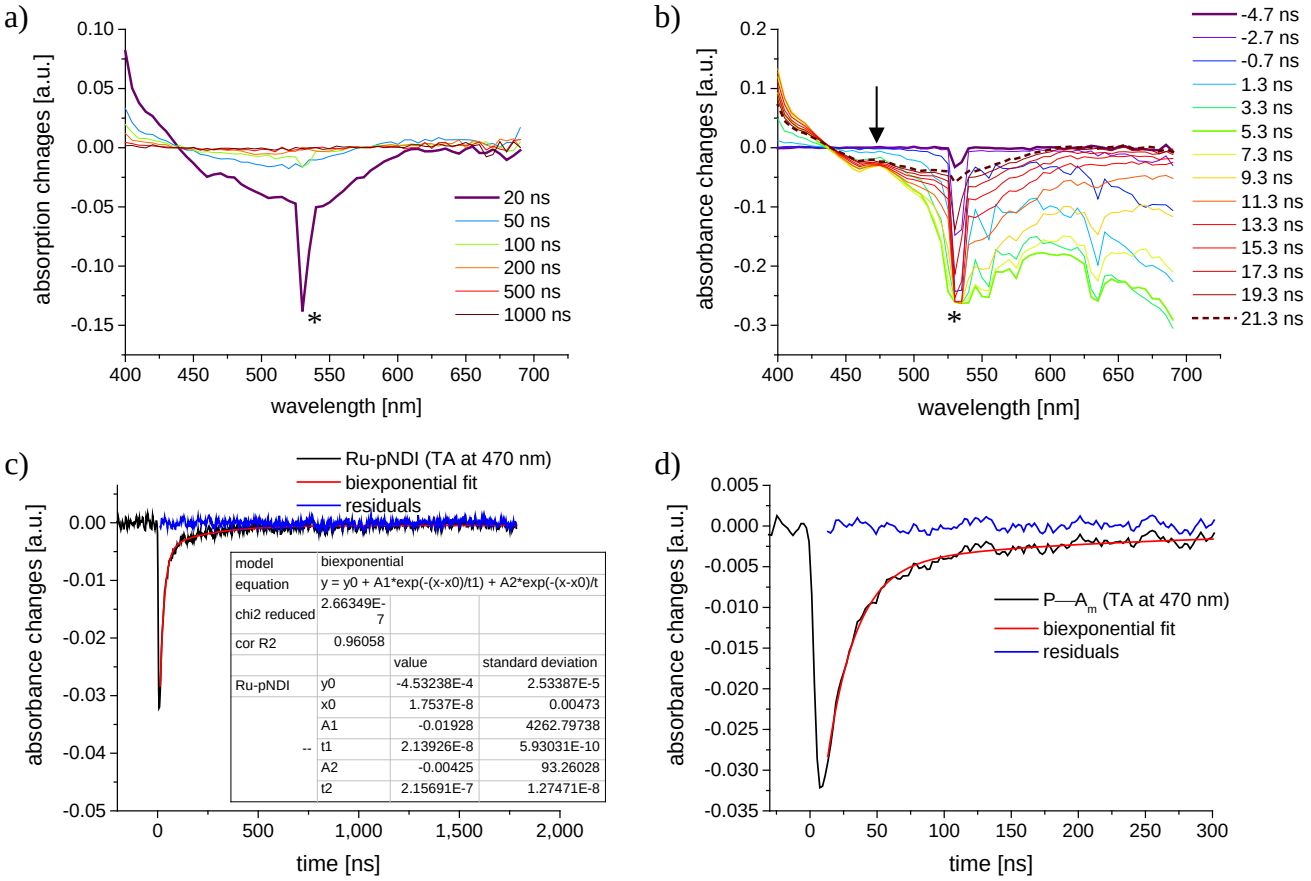

Figure S31. Transient absorption data of **P–A$_m$**: (a) Spectral recovery at selected times with zoom of pulse region (b). Note the preserved isosbestic point around 435 nm but clear deviation at 575 nm with respect to Ru (Figure S29), as well as the more negative TA signals between 575 and 650 nm assigned to additional polymer-based emission (see text). Note the very weak TA features of pNDI^{-} (475 nm) developing and decaying with excitation time window (maximal after 5.3 ns). After 21.3 ns, the typical ^{3}MLCT without polymer-emission is observed. Asterisk denotes excitation pulse artefacts including Rayleigh scatter. (c) Decay profile with fit at 470 nm and zoom to pulse region (d), corroborating the charge separation and rapid charge recombination.

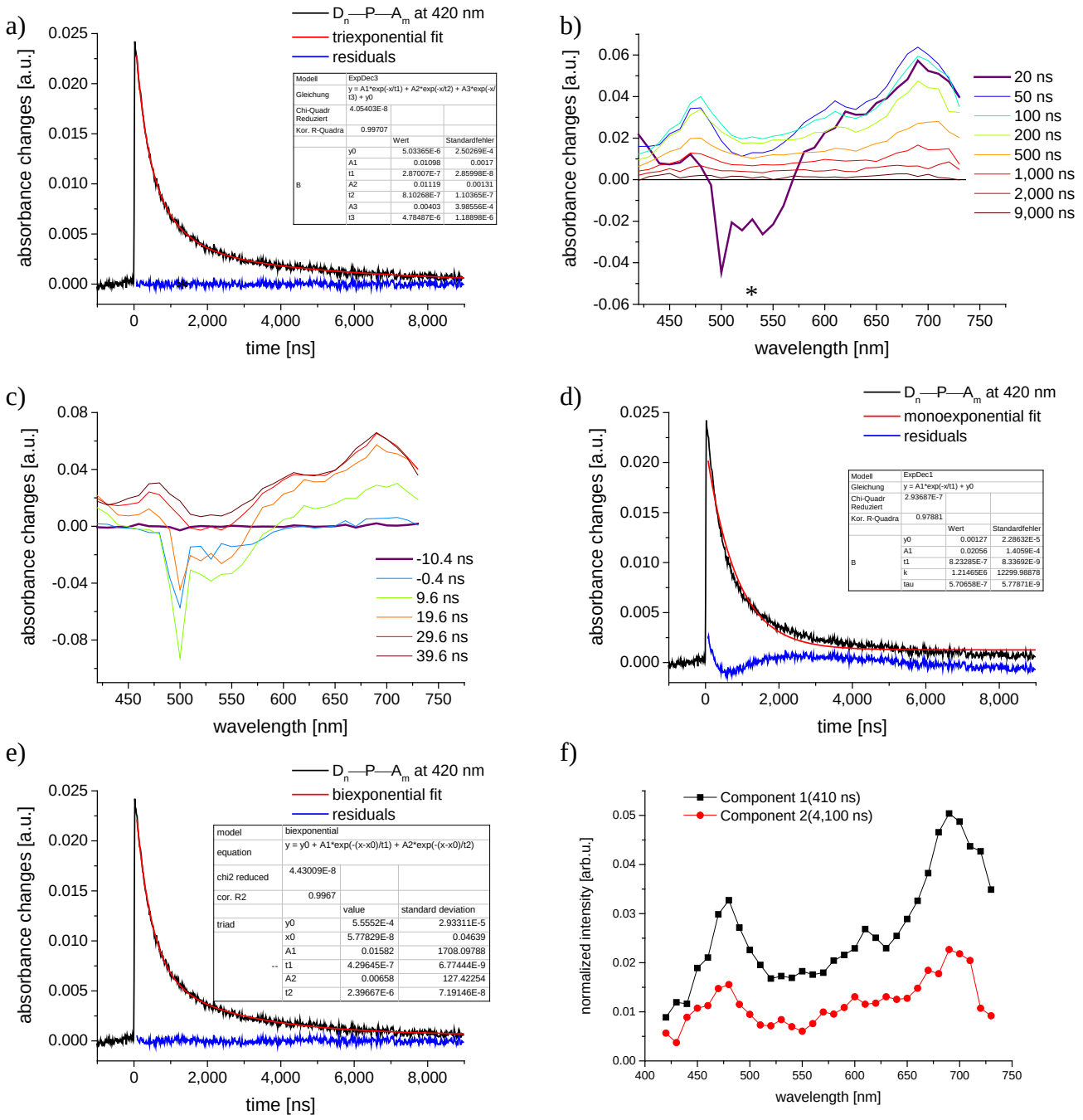

Figure S32. Transient absorption data of **D_n–P–A_m**: (a) Spectral recovery at selected times with zoom of pulse region (b). Asterisk denotes excitation pulse artefacts due to Rayleigh scatter. Note the rapid formation of positive TA signals with characteristic signatures of **pNDI$^-$** (475 and 610 nm) and **pTARA$^+$** (690 nm) in accordance to the spectroelectrochemical data. (c, d, e) Decay profile (at 420 nm) applying multiexponential fits: (c) Monoexponential, (d) biexponential and (e) triexponential fits with time constants of 430 ns (71%) and 2,400 ns (29%). (f) Global fit (> 100 ns) with biexponential kinetics with corresponding amplitudes. Component 1 (black curve) and 2 (red curve) shows similar spectral signatures of the fully charge separated state.

Table S2. Tabulated data of $\mathbf{D_n–P–A_m}$ from the mono-, bi- and triexponential fits with associated lifetimes and standard deviation, relative amplitudes.

	monoexponential	biexponential	triexponential
Component1	823 ± 8 ns (100%)	430 ± 7 ns (71%)	287 ± 28 ns (42%)
Component2	-	2,400 ± 72 ns (29%)	810 ± 110 ns (43%)
Component3	-	-	4,800 ± 1,100 ns (15%)
χ^2-reduced	2.937×E-7	4.430×E-8	4.054×E-8
Correlated R^2	0.9788	0.9967	0.9971

References

1. G. R. Fulmer, A. J. M. Miller, N. H. Sherden, H. E. Gottlieb, A. Nudelman, B. M. Stoltz, J. E. Bercaw and K. I. Goldberg, *Organometallics*, 2010, **29**, 2176-2179.
2. A. El-Zohry, A. Orthaber and B. Zietz, *J. Phys. Chem. C Nanomater. Interfaces*, 2012, **116**, 26144-26153.
3. Note the transmission characteristics of the "3C1 Russian Filter" given in Figure S25.
4. R. Schroot, C. Friebe, E. Altuntas, S. Crotty, M. Jäger and U. S. Schubert, *Macromolecules*, 2013, **46**, 2039-2048.
5. J. Kübel, R. Schroot, M. Wächtler, U. S. Schubert, B. Dietzek and M. Jäger, *J. Phys. Chem. C*, 2015, **119**, 4742-4751.
6. M. Jäger, R. J. Kumar, H. Görls, J. Bergquist and O. Johansson, *Inorg. Chem.*, 2009, **48**, 3228-3238.
7. M. Jäger, L. Eriksson, J. Bergquist and O. Johansson, *J. Org. Chem.*, 2007, **72**, 10227-10230.
8. R. Schroot, U. S. Schubert and M. Jäger, *Macromolecules*, 2015, **48**, 1963-1971.